Optics Letters

Generation of 1 kHz, 2.3 mJ, 88 fs, 2.5 μm pulses from a Cr^{2+}:ZnSe chirped pulse amplifier

Xiaoming Ren, Lam H. Mach, Yanchun Yin, Yang Wang, and Zenghu Chang*

Institute for the Frontier of Attosecond Science and Technology, CREOL and Department of Physics, University of Central Florida, Orlando, Florida 32816, USA
**Corresponding author: Zenghu.Chang@ucf.edu*

Received 21 May 2018; revised 15 June 2018; accepted 15 June 2018; posted 15 June 2018 (Doc. ID 332165); published 11 July 2018

We demonstrate the generation of 2.3 mJ, 88 fs, 2.5 μm laser pulses at 1 kHz repetition rate from a three-stage chirped pulse amplifier employing Cr^{2+}:ZnSe crystals as the active gain media. 5 μJ seed of the amplifier is obtained via intrapulse difference frequency generation in a bismuth triborate (BIBO) crystal from spectrally broadened Ti: Sapphire amplifier output. A multi-pass amplifier followed by two single-pass amplifiers pumped by *Q*-switched Ho:YAG lasers boost the pulse energy to 6.5 mJ, yielding 2.3 mJ, 88 fs pulses upon pulse compression. Our results show the highest peak power at 2.5 μm with 1 kHz repetition rate. Such a laser will be a powerful source for studying strong-field physics and extending high-harmonic generation towards the keV region.

OCIS codes: (140.3070) Infrared and far-infrared lasers; (140.5680) Rare earth and transition metal solid-state lasers; (320.7090) Ultrafast lasers.

https://doi.org/10.1364/OL.43.003381

In recent years, there has been an upsurge in the demand for high-energy, multi/few-cycle lasers in the short- (SWIR) to mid-wave infrared (MWIR) spectral regions. Aside from their important applications in molecular spectroscopy [1] and remote sensing [2], these long-wavelength lasers have also demonstrated great potential in the study of strong-field physics and attosecond science [3–12], especially in extending high-harmonic generation (HHG) beyond the water window and towards the keV region [13,14]. Generating such long-wavelength lasers typically requires a Ti:Sapphire frontend, seed generation via spectral broadening [15] or difference frequency generation (DFG) [16], energy upscaling via optical parametric amplification (OPA) [8,17,18] or optical parametric chirped pulse amplification (OPCPA) [16,19–21], and finally necessary spectral broadening and pulse compression if few-cycle pulses are needed [17]. By utilizing these techniques, mJ-level, few-cycle lasers operating in the kHz regime have been demonstrated with the center wavelength extended as far as 5.1 μm [22].

An alternative and more effective way of generating high-energy multi/few-cycle long-wavelength lasers is through chirped pulse amplification (CPA) [23], a technique that has enabled high-energy Ti:Sapphire lasers—the workhorse in ultrafast science and industry for the past two decades. Essential ingredients for implementing CPA include a gain medium possessing a broad emission spectrum with high quantum efficiency, and a high-energy pump source with nanosecond (ns) pulse duration. Thanks to the rapid development of high-quality transition-metal-doped II-VI semiconductors and associated fiber-laser-pumped *Q*-switched Ho:YAG and Er:YAG lasers, Ti:Sapphire CPA technique can now find its equivalence in the SWIR and MWIR regions, with Cr^{2+}:ZnSe/ZnS and Fe^{2+}:ZnSe/ZnS used as the gain medium, respectively [24–26]. While the development of Cr^{2+}:ZnSe/ZnS oscillators has seen rapid progress in recent years [26], there are only a few reports on Cr^{2+}:ZnSe/ZnS amplifiers operating in the kHz regime with the highest energy of 1 mJ achieved by *Q*-peak Inc [27]. However, the pulse duration was limited to 184 fs, mainly due to gain narrowing effect with a nJ level seed from a Cr^{2+}:ZnSe oscillator.

In this Letter, we report on the construction of a 2.3 mJ, 88 fs, 2.5 μm Cr^{2+}:ZnSe CPA laser operating at 1 kHz repetition rate. The high pulse energy and short pulse duration are enabled by using a μJ-level ultra-broadband seed laser [28]. To the best of our knowledge, this result represents the highest peak power ever achieved at 2.5 μm with 1 kHz repetition rate.

The laser layout is illustrated in Fig. 1. Its frontend features a home-built Ti:Sapphire CPA laser generating 1.2 mJ and 30 fs pulses at a repetition rate of 1 kHz. These pulses are loosely focused by a 2 m focal length lens into a stretched hollow-core fiber (HCF) filled with 3 bar of neon gas for white light generation [29]. The HCF is a polyimide-coated flexible

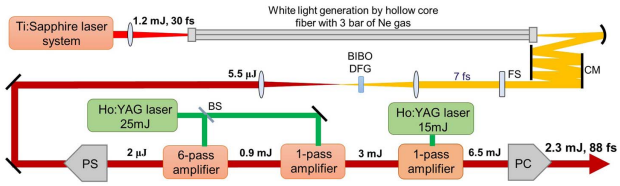

Fig. 1. Schematic layout of the Cr^{2+}:ZnSe CPA laser. CM, chirped mirrors; FS, fused silica compensation plate; DFG, difference frequency generation; PS, pulse stretcher; PC, pulse compressor.

fused-silica capillary tubing with 500 μm inner diameter and 1.5 m length. Sets of chirped mirrors and fused-silica plates are used to compress the HCF output to around 7 fs, which is then focused into a 0.8 mm bismuth triborate (BIBO) crystal cut at 10.3° for intrapulse DFG. The crystal is cut for Type I phase matching, and the *e* axis of the crystal is rotated 8° away from the HCF output polarization to allow a maximum DFG output of 5.5 μJ following a cascade process [28]. The DFG output has an octave-spanning spectrum covering from 1.6 μm to around 3.6 μm with a nice Gaussian beam profile, as shown in Fig. 2. Note that an alternative white light generation method such as using filamentation tube [30] and condensed medium [31,32] can also be adopted with less susceptibility to beam pointing change, given that they can provide adequate bandwidth for DFG.

The DFG output is used as the seed for the Cr^{2+}:ZnSe CPA laser. As in the standard CPA architecture, the seed is first stretched to about 300 ps in an all-reflective Offner-type pulse stretcher. The stretcher employs a ruled reflective grating with a 300 l/mm groove density and gives a 2 μJ output whose spectrum is truncated between 2.2 μm and 3 μm (see Fig. 2) due to limited retro-reflective mirror size in the stretcher. Note that the output spectral range can be easily tuned by changing the angle of the grating, and this specific range is chosen to overlap with the peak of the emission spectrum of the Cr^{2+}:ZnSe crystal [24] as well as mitigating strong absorption of the gain crystal below 2.2 μm.

The first-stage multi-pass amplifier employs a 30 mm-long, Brewster-angle-cut (67.7°) polycrystalline Cr^{2+}:ZnSe crystal (IPG Photonics Inc.) having a 95% absorption at 2.09 μm. A Tm-fiber laser-pumped, *Q*-switched Ho:YAG laser at 2.09 μm with 25 mJ pulse energy at 1 kHz (IPG Photonics Inc.) is used as the pump laser for the amplifier. Fifty percent of the total energy (12 mJ) is focused to the crystal with a spot size of around 1.2 mm overlapping with the 1 mm seed at focus. The seed is refocused back into the crystal after each pass to maintain a constant spot size. After six passes, 900 μJ of pulse

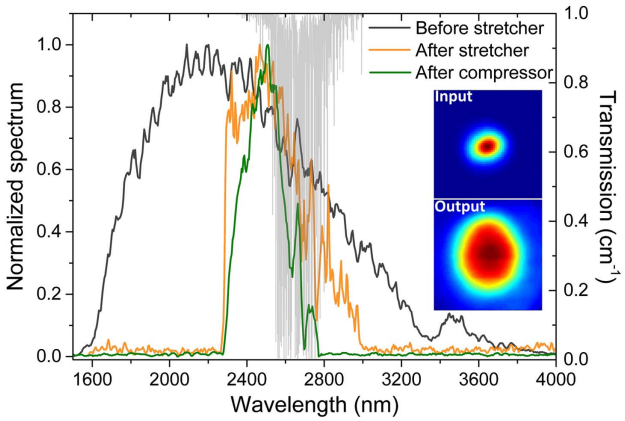

Fig. 2. Power spectrum and spatial profile of the laser before and after the Cr^{2+}:ZnSe CPA system. Black curve shows the seed spectrum after the DFG. Orange curve denotes the laser spectrum after the stretcher. Green curve represents the final output laser spectrum after the pulse compressor. Shaded gray lines on the top axis show the power transmission through 1 cm of water vapor at normal condition. Insets show the input and output beam profiles measured with Spiricon Pyrocam IIIHR beam profiling camera.

energy is achieved with a cumulative gain of 450. The first-stage output is then resized to around 2 mm and sent to the second-stage amplifier employing a 40 mm-long polycrystalline Cr^{2+}:ZnSe rectangular slab. The crystal absorbs 99% of the pump power and is anti-reflection coated from 1.9 μm to 3 μm. The remainder of the first-stage pump (12 mJ) is sent to the second-stage crystal with a spot size of 2 mm and boosts the energy to 3 mJ with a single pass. Strong thermal lensing effect causes the output to focus after the crystal. To prevent optical damage, the second-stage output is picked off after the focus, resized to 2.5 mm, and sent to the third-stage crystal (same as the second-stage crystal). Another Tm-fiber laser-pumped, *Q*-switched Ho:YAG laser at 2.09 μm with 50 mJ pulse energy at 1 kHz (IPG Photonics Inc.) is used to pump the last stage. With 15 mJ pumping energy and 2.5 mm pump size, 6.5 mJ output energy is achieved with one pass. Further increasing the pump energy leads to gain saturation. Enlarging the pump and seed beam size would allow for more pump energy to be stored in the gain crystal, potentially leading to higher output energy with a chance of introducing thermally induced spatial distortion on the pump beam along with other thermal problems [33]. Novel techniques such as using spinning ring gain medium [34] will be needed to greatly boost the output power. Note that all crystals are water-cooled to 15°C.

Finally, to avoid damaging the compressor gratings, the amplifier output is resized to 10 mm and sent to the pulse compressor consisting of two ruled reflective gratings with 300 l/mm groove density. Considering surface losses along the beam path from the third-stage output, the compressor throughput efficiency is estimated to be around 60% yielding 3 mJ of pulse energy at the exit. The spectrum of the final output is shown in Fig. 2 along with its superb spatial profile. The spectrum is narrower than the input, which can be attributed to the crystal absorption at the shorter wavelength side and strong water vapor absorption at the longer wavelength side. A broader spectrum is expected by purging the entire system with dry air or nitrogen. The absorption of the crystal can be mitigated at the cost of slightly reduced output power by tuning the angle of the stretcher grating shifting the seeding spectrum towards longer wavelengths while purging. Nevertheless, the output spectrum can support a transform-limited (TL) pulse duration of 40 fs, corresponding to five-cycle pulses at 2.5 μm.

To measure the pulse duration, a single-shot second-harmonic frequency-resolved optical gating (SH-FROG) measurement is performed by splitting the output beam spatially into two halves and cross overlapping the split portions in a 100 μm-thick beta-barium borate (BBO) crystal cut for 2.5 μm. The measured and retrieved FROG traces are shown with very good agreement in Figs. 3(a) and 3(b), respectively. Note that the SH bandwidth extends only to around 1240 nm (corresponding to 2480 nm of the fundamental spectrum), which is much lower than the upper limit of the measured fundamental spectrum. This is due to the strong water absorption at the red side of the spectrum that severely distorts the spectral phase causing the spectral region above 2480 nm to be uncompressible. To prevent discrepancy between measured and retrieved spectra as well as to get the real compressed pulse energy, a slit is placed in the compressor as a spectral filter to block the uncompressible portion of the spectrum while keeping the FROG spectrogram unchanged. The red curve in Fig. 3(c) shows the measured spectrum after spectral filtering. The measured

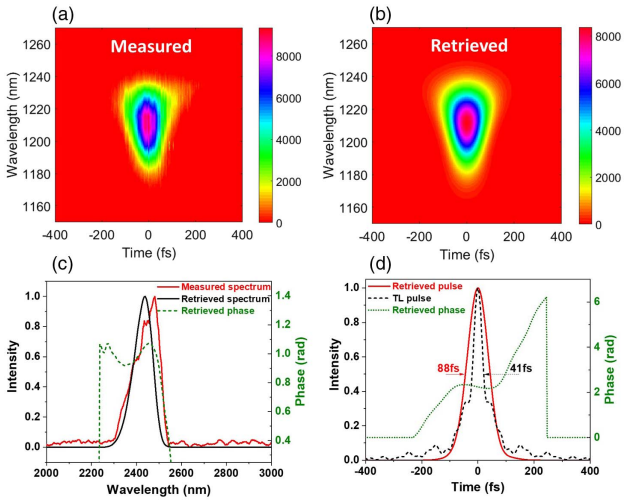

Fig. 3. FROG measurement and retrieval. (a) Measured FROG trace. (b) Retrieved FROG trace. (c) Red curve, measured spectrum with spectral filtering (see text for more detail); black curve, retrieved spectrum; green dashed curve, retrieved spectral phase. (d) Red curve, retrieved pulse intensity profile; green dotted curve, retrieved temporal phase; black dashed curve, transform limited pulse supported by the clipped spectrum [red curve in panel (c)].

and retrieved spectra are in good agreement, indicating a reliable retrieval with a retrieved pulse duration of 88 fs. The corresponding pulse energy drops from 3 mJ to 2.3 mJ, indicating a peak power of 26 GW at 1 kHz. The pulse duration and peak power are expected to improve further once the entire laser system is purged.

It is also worth mentioning that our seed laser is generated from an intrapulse DFG process, which provides passive carrier–envelope-phase (CEP) stability [35]. The final output should inherit such stability, which makes our laser source extremely valuable to the field of attosecond science. Although it is well known that a grating-based stretcher and compressor can introduce large noise to the CEP [36], the CEP stability needs to be measured, and active feedback controls are necessary to provide a stable CEP output.

To conclude, we have demonstrated, to the best of our knowledge, the highest peak power at 2.5 μm with a 2.3 mJ pulse energy and 88 fs pulse duration operating at 1 kHz. Such a laser is enabled by a μJ level broadband seed laser followed by a three-stage Cr^{2+}:ZnSe CPA laser. In the field of attosecond science, the generated harmonic cutoff scales quadratically with the driving laser's wavelength λ [37]; meanwhile, the single atom response for generating high-energy photons drastically drops as $\lambda^{-5\sim-6}$ [38]. The high peak power of our laser at 2.5 μm could be a powerful source in the generation of high-flux attosecond pulses with photon energy extending beyond the water window and towards the keV region.

Funding. Army Research Office (ARO) (W911NF-14-1-0383); Air Force Office of Scientific Research (AFOSR) (FA9550-15-1-0037, FA9550-16-1-0013, FA9550-17-1-0499); Defense Advanced Research Projects Agency (DARPA) (W31P4Q1310017).

REFERENCES

1. F. K. Tittel, D. Richter, and A. Fried, "Mid-infrared laser applications in spectroscopy," in *Solid-State Mid-Infrared Laser Sources* (Springer, 2003), pp. 458–529.
2. P. Werle, F. Slemr, K. Maurer, R. Kormann, R. Mücke, and B. Jänker, Opt. Lasers Eng. **37**, 101 (2002).
3. Z. Chang, P. B. Corkum, and S. R. Leone, J. Opt. Soc. Am. B **33**, 1081 (2016).
4. B. Wolter, M. G. Pullen, M. Baudisch, M. Sclafani, M. Hemmer, A. Senftleben, C. D. Schröter, J. Ullrich, R. Moshammer, and J. Biegert, Phys. Rev. X **5**, 021034 (2015).
5. H. Xiong, H. Xu, Y. Fu, J. Yao, B. Zeng, W. Chu, Y. Cheng, Z. Xu, E. J. Takahashi, K. Midorikawa, X. Liu, and J. Chen, Opt. Lett. **34**, 1747 (2009).
6. N. Ishii, K. Kaneshima, K. Kitano, T. Kanai, S. Watanabe, and J. Itatani, Nat. Commun. **5**, 3331 (2014).
7. E. J. Takahashi, T. Kanai, K. L. Ishikawa, Y. Nabekawa, and K. Midorikawa, Phys. Rev. Lett. **101**, 253901 (2008).
8. A. Johnson, L. Miseikis, D. Wood, D. Austin, C. Brahms, S. Jarosch, C. Strüber, P. Ye, and J. Marangos, Struct. Dyn. **3**, 062603 (2016).
9. S. Teichmann, F. Silva, S. Cousin, M. Hemmer, and J. Biegert, Nat. Commun. **7**, 11493 (2016).
10. M.-C. Chen, P. Arpin, T. Popmintchev, M. Gerrity, B. Zhang, M. Seaberg, D. Popmintchev, M. Murnane, and H. Kapteyn, Phys. Rev. Lett. **105**, 173901 (2010).
11. G. J. Stein, P. D. Keathley, P. Krogen, H. Liang, J. P. Siqueira, C. L. Chang, C. J. Lai, K. H. Hong, G. M. Laurent, and F. X. Kärtner, J. Phys. B **49**, 155601 (2016).
12. T. Popmintchev, M. C. Chen, D. Popmintchev, P. Arpin, S. Brown, S. Alisauskas, G. Andriukaitis, T. Balciunas, O. D. Mücke, A. Pugzlys, A. Baltuska, B. Shim, S. E. Schrauth, A. Gaeta, C. Hernández-García, L. Plaja, A. Becker, A. J. Becker, M. M. Murnane, and H. C. Kapteyn, Science **336**, 1287 (2012).
13. J. Li, X. Ren, Y. Yin, K. Zhao, A. Chew, Y. Cheng, E. Cunningham, Y. Wang, S. Hu, Y. Wu, M. Chini, and Z. Chang, Nat. Commun. **186**, 8 (2017).
14. X. Ren, J. Li, Y. Yin, K. Zhao, A. Chew, Y. Wang, S. Hu, Y. Cheng, E. Cunningham, Y. Wu, M. Chini, and Z. Chang, J. Opt. **20**, 023001 (2018).
15. D. Brida, C. Manzoni, G. Cirmi, M. Marangoni, S. Bonora, P. Villoresi, S. De Silvestri, and G. Cerullo, J. Opt. **12**, 013001 (2009).
16. Y. Yin, J. Li, X. Ren, K. Zhao, Y. Wu, E. Cunningham, and Z. Chang, Opt. Lett. **41**, 1142 (2016).
17. B. E. Schmidt, P. Béjot, M. Giguère, A. D. Shiner, C. Trallero-Herrero, É. Bisson, J. Kasparian, J.-P.Wolf, D. M. Villeneuve, J.-C. Kieffer, P. B. Corkum, and F. Légaré, Appl. Phys. Lett. **96**, 121109 (2010).
18. S. Cousin, F. Silva, S. Teichmann, M. Hemmer, B. Buades, and J. Biegert, Opt. Lett. **39**, 5383 (2014).
19. N. Ishii, K. Kaneshima, K. Kitano, T. Kanai, S. Watanabe, and J. Itatani, Opt. Lett. **37**, 4182 (2012).
20. Y. Deng, A. Schwarz, H. Fattahi, M. Ueffing, X. Gu, M. Ossiander, T. Metzger, V. Pervak, H. Ishizuki, T. Taira, T. Kobayashi, G. Marcus, F. Krausz, R. Kienberger, and N. Karpowicz, Opt. Lett. **37**, 4973 (2012).
21. K.-H. Hong, C.-J. Lai, J. P. Siqueira, P. Krogen, J. Moses, C.-L. Chang, G. J. Stein, L. E. Zapata, and F. X. Kärtner, Opt. Lett. **39**, 3145 (2014).
22. L. von Grafenstein, M. Bock, D. Ueberschaer, K. Zawilski, P. Schunemann, U. Griebner, and T. Elsaesser, Opt. Lett. **42**, 3796 (2017).
23. P. Maine, D. Strickland, P. Bado, M. Pessot, and G. Mourou, IEEE J. Quantum Electron. **24**, 398 (1988).
24. I. T. Sorokina and E. Sorokin, IEEE J. Sel. Top. Quantum Electron. **21**, 273 (2015).
25. S. B. Mirov, V. V. Fedorov, D. Martyshkin, I. S. Moskalev, M. Mirov, and S. Vasilyev, IEEE J. Sel. Top. Quantum Electron. **21**, 292 (2015).
26. S. Mirov, I. Moskalev, S. Vasilyev, V. Smolski, V. Fedorov, D. Martyshkin, J. Peppers, M. Mirov, A. Dergachev, and V. Gapontsev, IEEE J. Sel. Top. Quantum Electron. (2018).
27. E. Slobodchikov, L. R. Chieffo, and K. F. Wall, Proc. SPIE **9726**, 972603 (2016).

28. Y. Yin, X. Ren, A. Chew, J. Li, Y. Wang, F. Zhuang, Y. Wu, and Z. Chang, Sci. Rep. **7**, 11097 (2017).
29. V. Cardin, N. Thiré, S. Beaulieu, V. Wanie, F. Légaré, and B. E. Schmidt, Appl. Phys. Lett. **107**, 181101 (2015).
30. C. Hauri, W. Kornelis, F. Helbing, A. Heinrich, A. Couairon, A. Mysyrowicz, J. Biegert, and U. Keller, Appl. Phys. B **79**, 673 (2004).
31. C.-H. Lu, Y.-J. Tsou, H.-Y. Chen, B.-H. Chen, Y.-C. Cheng, S.-D. Yang, M.-C. Chen, C.-C. Hsu, and A. H. Kung, Optica **1**, 400 (2014).
32. P. He, Y. Liu, K. Zhao, H. Teng, X. He, P. Huang, H. Huang, S. Zhong, Y. Jiang, S. Fang, X. Hou, and Z. Wei, Opt. Lett. **42**, 474 (2017).
33. I. Moskalev, V. Fedorov, and S. Mirov, Opt. Express **17**, 2048 (2009).
34. I. Moskalev, S. Mirov, M. Mirov, S. Vasilyev, V. Smolski, A. Zakrevskiy, and V. Gapontsev, Opt. Express **24**, 21090 (2016).
35. A. Baltuška, T. Fuji, and T. Kobayashi, Phys. Rev. Lett. **88**, 133901 (2002).
36. C. Li, E. Moon, and Z. Chang, Opt. Lett. **31**, 3113 (2006).
37. B. Shan and Z. Chang, Phys. Rev. A **65**, 011804 (2001).
38. A. Shiner, C. Trallero-Herrero, N. Kajumba, H.-C. Bandulet, D. Comtois, F. Légaré, M. Giguère, J. Kieffer, P. Corkum, and D. Villeneuve, Phys. Rev. Lett. **103**, 073902 (2009).